

Lasers in Manufacturing Conference 2021

Combining LPBF and ultrafast laser processing to produce parts with deep microstructures

Manuel Henn^{a,*}, Matthias Buser^a, Volker Onuseit^a, Rudolf Weber^a, Thomas Graf^a

^aInstitut für Strahlwerkzeuge (IFSW), Pfaffenwaldring 43, 70569 Stuttgart, Germany

Abstract

Laser Powder Bed Fusion (LPBF) is limited in the achievable accuracy, surface quality and structure size due to its inherent melting process. The achievable structure sizes are mainly dependent on the focal diameter and the grain size of the powder. Smaller structures, especially deep and narrow slits with a width below 100 μm , are still a major challenge. Combining continuous wave and ultrashort pulsed lasers in the same optical system enables consecutive additive and subtractive processes. This results in a quasi-simultaneous manufacturing process, where the emerging part can be precisely machined with ultrafast laser ablation after each additively added layer. In the talk the system technology used for the superposition of the lasers as well as the results of the combined additive and subtractive processes for the fabrication of deep and narrow slits in stainless steel parts will be shown.

Keywords: laser powder bed fusion; ultrafast laser ablation; additive manufacturing; microstructures

1. Introduction

LPBF is an additive manufacturing process for the production of highly complex parts characterized by the melting of multiple fused beads in subsequent layers of metal powder. The achievable precision is a function of the used process parameters, mainly the diameter of the laser beam d_f on the surface, typically in the range of 50 – 500 μm , and the feed rate and laser power which define the width of the melted area. Small topological structures such as internal slits with a width of about 100 μm and larger can be achieved by increasing the distance between scanned lines. Similar to the achievable qualities of free surfaces, the achievable accuracy in the generation of the small structures is limited. The main issue is the lack of contour sharpness as a result of the melting process, as shown by Yasa et al., 2011. This effect can be compensated by using even smaller focal diameters and finer powders as summarized by Liu et al., 2011 and Ziri et al., 2021. However, for internal

* Corresponding author. Tel.: +49 711 685 61509
E-mail address: manuel.henn@ifsw.uni-stuttgart.de

powder free structures the powder size has to be larger than the structure size. Smaller structures, especially deep and narrow grooves or slits with a width below $100\ \mu\text{m}$ are therefore still a major challenge. This is particularly true when the structures are required inside the bulk material without access from the outside, as is the case in additive manufacturing of soft magnetic materials, which was demonstrated by Goll et al., 2019. However, structures in metals and semiconductors within the range of $100\ \mu\text{m}$ and below can be easily created by a multi-pass ablation strategy using ultrafast lasers, as described by Fornaroli et al., 2013. To exceed the current limitations on narrow slit width, a concept from Ghosh et al., 2018, is adapted to combine continuous wave LPBF and ultrafast laser ablation in one processing system. The two lasers are integrated into the same optical path, enabling a quasi-simultaneous manufacturing process, consisting of consecutive additive and subtractive laser processes.

2. Experimental setup

The experimental setup, shown in Fig. 1, consists of a custom built powder bed, a galvanometer scanner with f-theta lens, and two laser sources combined in one optical path with flip mirror, all integrated in a flexible multi-axis processing station for integrated control of all systems. For the LPBF process, a thin-disk laser with a delivery fiber with a core diameter of $100\ \mu\text{m}$ was used in conjunction with a collimating lens of $75\ \text{mm}$ focal length to couple the laser beam into the current system. For the laser structuring process an ultrafast laser with a pulse duration of $8\ \text{ps}$ and a raw beam parameter of $6\ \text{mm}$ was used. Both laser sources were operated with a wavelength λ of $1030\ \text{nm}$. The detailed parameters of the two laser sources used for this investigation are listed in Table 1. To enable an efficient switching between the two laser sources, the system was expanded to include a pneumatically switchable flip mirror. This enables fast switching and full integration into the existing safety concept of the laser machining system. Since both laser sources share the same wavelength of $1030\ \text{nm}$, they can also be coupled into the same focusing optics. In this case, both beams were focused on the part by a galvanometer scanning head in combination with a f-Theta lens with a focal length of $163\ \text{mm}$. The realized focal diameters of the cw-source and the ultrafast source were approx. $d_{f,cw} = 190\ \mu\text{m}$ and $d_{f,usp} = 50\ \mu\text{m}$ respectively. The scanning head could be moved vertically using a translation stage to ensure that each focal point of the laser beams was set onto the build plane for each individual process, allowing for the smallest feasible feature sizes.

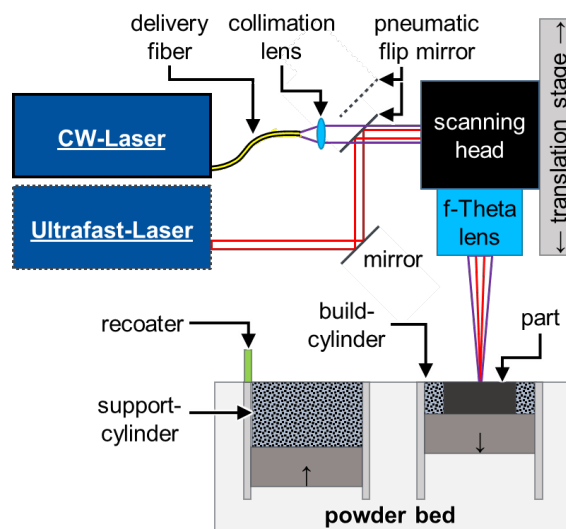


Fig. 1. Schematic illustration of the experimental setup.

Table 1: Parameters of the used laser systems.

CW-Laser		
Wavelength	λ	1030 nm
Average power	P	8 kW
Delivery fibre diameter		100 μm
Beam Quality	M^2	≤ 11
Raw beam diameter	D_r	12 mm
Polarization		Linear
Ultrafast-Laser		
Wavelength	λ	1030 nm
Average power	P	65 W
Max. pulse energy	E_p	$\leq 215 \mu\text{J}$
Repetition rate	f_{rep}	$\leq 300 \text{ kHz}$
Pulse duration	τ	8 ps
Beam Quality	M^2	< 1.4
Raw beam diameter	D_r	6 mm
Polarization		Linear

2.1 Additive Process

An average power of 700 W and a scanning speed of 1 m/s was used for the melting of the metal powder. In this case stainless steel 630A (1.4542) with an average particle size of 30 μm was used. The custom build powder bed provides heating ability of the build plate, whereas the temperature was set to 200°C. The height of the powder layer was set constant to 50 μm . A cross jet was used to prevent spatters to reach the laser optics. Nitrogen was used as shielding gas during the process. The smallest feasible melt bead with a width of approx. 200 μm was achieved in focal position.

2.2 Subtractive Process

Using an average power of 30 W and a pulse energy of 100 μJ at a repetition rate of 300 kHz and a scanning speed of 3 m/s resulting in a pulse overlap of 80%, lines with a length of 5 mm were ablated after each consecutive powder layer was welded to the part. The number of repetitions for each line was set to 3000.

3. Results

The consecutive process steps, LPBF and structuring, described above were repeated for a number of 20 layers resulting in a part with a cumulative height of approx. 1 mm above the base plate. In Fig. 2 a cross-section perpendicular to scanning direction of the ablated lines is shown. Apart from some transversal bulges, the average slit width is approx. 50 μm . Due to the sample preparation for imaging, it appears that the last upper layer is closed. However, all added layers were cut through, since the subtractive process was performed last in this example. Although the slit width is larger than the average particle size of the powder, no residual particles were observed within the slits. The average total depth of the slots is about 1.3 mm, resulting in an aspect ratio of height to width of about 26:1.

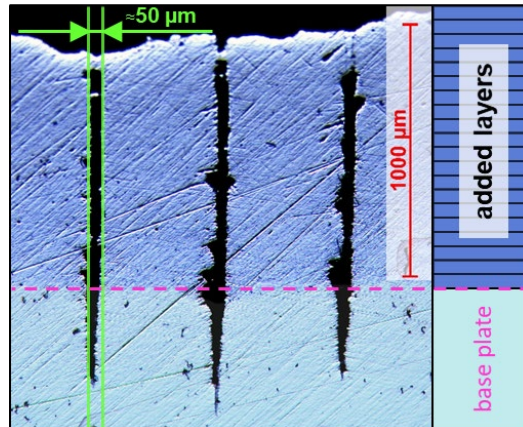


Fig. 1. Cross-section of a sample with 20 layers of consecutive additive and subtractive laser processes. The average slit-width is approx. $50\ \mu\text{m}$ with a maximum depth of approx. $1.3\ \text{mm}$.

4. Conclusion

In summary, it is possible to combine additive and subtractive laser-based processes into one consecutive process. In a first experiment it was possible to cut narrow slits with a width of about $50\ \mu\text{m}$ over a total of 20 additive layers, resulting in a maximum slit depth of about $1.3\ \text{mm}$ and an aspect ratio of approx. 26:1. At this stage of the investigations, no principal limits for the achievable aspect ratio were found.

References

- Liu, B., Wildman, R., Tuck, C., Ashcroft, I., Hague, R., 2011. „Investigation the Effect of Particle Size Distribution on Processing Parameters Optimisation in Selective Laser Melting Process”.
- Fornaroli C., Holtkamp J., Gillner A., 2013. „Dicing of thin Si wafers with a picosecond laser ablation process”, Lasers in Manufacturing Conference, p. 603–609.
- Ghosh, A., Wang, X., Kietzig, A.-M., Brochua, M., 2018. „Layer-by-layer combination of laser powder bed fusion (LPBF) and femtosecond laser surface machining of fabricated stainless steel components”, Journal of Manufacturing Processes 35, p. 327–336.
- Goll, D., Schuller, D., Martinek, G., Kunert, T., Schurr, J., Sinz, C., Schubert, T., Bernthaler, T., Riegel, H., Schneider, G., 2019. „Additive manufacturing of soft magnetic materials and components”, Addit. Manuf. 27, p. 428–439.
- Yasa, E., Kruth, J.-P., Deckers, J., 2011. „Manufacturing by combining Selective Laser Melting and Selective Laser Erosion/laser re-melting”, CIRP Annals - Manufacturing Technology 60, p. 263–266.
- Ziri, S., Hor, A., Mabru, C., 2021. „Effect of powder size and processing parameters on surface, density and mechanical properties of 316L elaborated by Laser Powder Bed Fusion”, ESAFORM MS13 (AM), 10.25518/esaform21.1563.